Uncorrected Proof

Shiraz E-Med J. 2026 July; 27(7): e173453 https://doi.org/10.5812/semj-173453

Published Online: 2026 July 31 **Research Article**

Brimonidine Induces Pro-apoptotic and Inflammatory Transcriptional Responses in Human Corneal Keratocytes: An in vitro and in silico Network Analysis

Azadeh Samaeili [1], Fatemeh Sanie-Jahromi [2], Mehrnaz Soltaninejad [1], Abbas Mohammadi [1], Rozhin Kasiri [1], Maryam Adabi [3,*]

[1] Infectious Ophthalmologic Research Center, Ahvaz Jundishapur University of Medical Sciences, Ahvaz, Iran
[2] Department of Ophthalmology, Poostchi Ophthalmology Research CenterSchool of Medicine, Shiraz University of Medical Sciences, Shiraz, Iran
[3] Research Center for FoodHygiene and Safety, School of Public Health, Shahid Sadoughi University of Medical Sciences, Yazd, Iran

[*] ***Corresponding Author:*** Research Center for Food Hygiene and Safety, School of Public Health, Shahid SadoughiUniversity of Medical Sciences, Yazd, Iran. Email: maryam_adabi@yahoo.com

Received: 21 June, 2026; **Revised:** 4 July, 2026; **Accepted:** 15 July, 2026

Abstract

Background: Keratocytes maintain corneal transparency; their depletion causes scarring and vision loss.

Objectives: This study evaluated the cytotoxic effects of a commercial brimonidine formulation on primary human keratocytes by assessing the expression of genes involved in cell death.

Methods: Primary human keratocytes from a single donor were treated with 10 μM brimonidine tartrate. Cell viability was assessed using an MTT assay, and BAX, BCL2, and IL1B expression was assessed using real-time PCR. An in silico protein-protein interaction network analysis of apoptosis and pyroptosis pathways was conducted using STRING and Cytoscape. Experiments were performed in three biological replicates (n = 3) from a single donor. Statistical comparisons were performed using an unpaired t-test in GraphPad Prism (version 6).

Results: The brimonidine formulation significantly reduced keratocyte viability (73.81% vs. 100%, P = 0.0007) and upregulated BAX (P = 0.0078) and IL1B (P = 0.0268). The BCL2/BAX ratio showed a decreasing trend but did not reach significance (P = 0.0641).

Conclusions: The commercial brimonidine formulation exerts significant cytotoxicity in keratocytes and upregulates BAX and IL1B, suggesting transcriptional changes consistent with apoptotic and inflammatory signaling. However, these findings are preliminary and donor-specific and require validation in cells from multiple donors, as well as direct evidence of cell death mechanisms. The results raise questions about the long-term corneal effects of brimonidine-containing formulations.

Keywords: Corneal Keratocytes, Brimonidine Tartrate, Apoptosis, Pyroptosis, Glaucoma

1. Background

Brimonidine is an α2-adrenergic agonist widely used as a first-line treatment for lowering intraocular pressure (IOP) in patients with open-angle glaucoma and ocular hypertension (1). Its therapeutic effect is mediated through α2-adrenergic receptors in the ciliary body, where it suppresses aqueous humor production and enhances uveoscleral outflow (2). Despite its efficacy, topical brimonidine administration is frequently associated with adverse effects, including ocular discomfort, allergic reactions, and blurred vision (3). While some studies have highlighted potential neuroprotective roles for brimonidine in retinal cells (4, 5), its effect on the avascular cornea—the tissue first and most directly exposed to the drug—has been insufficiently explored.

The structural and optical integrity of the eye depends on the cornea, which in turn relies on a healthy population of keratocytes. These stromal cells are essential for synthesizing the extracellular matrix, maintaining corneal

Copyright © 2026, Samaeili et al. This open-access article is available under the Creative Commons Attribution 4.0 (CC BY 4.0) International License (https://creativecommons.org/licenses/by/4.0/), which allows for unrestricted use, distribution, and reproduction in any medium, provided that the original work is properly cited.

How to Cite: Samaeili A, Sanie-Jahromi F, Soltaninejad M, Mohammadi A, Kasiri R, et al. Brimonidine Induces Pro-apoptotic and Inflammatory Transcriptional Responses in Human Corneal Keratocytes: An in vitro and in silico Network Analysis. Shiraz E-Med J. 2026;27(7):e173453. doi: https://doi.org/10.5812/semj-173453

transparency, and mediating wound healing (6, 7). Disruption of keratocyte homeostasis is a known pathological process that can lead to corneal opacity, scar formation, and chronic ocular pain (8). Brimonidine penetrates the corneal cellular layers (9), and although the initial dose is rapidly cleared from the corneal surface, the underlying cell layers may remain exposed to the drug for a prolonged period. Given that topically administered ophthalmic drugs can exert significant off-target effects, understanding the potential cytotoxicity of brimonidine is essential to ensure patient safety and optimize clinical management.

2. Objectives

This study aimed to evaluate the effects of a commercial brimonidine tartrate ophthalmic formulation on cell viability and gene expression in primary human corneal keratocytes. Specifically, we focused on genes central to apoptosis (BCL2 and BAX) and the pyroptosis-associated inflammatory cytokine IL1B. Examining these molecular responses provides preliminary insight into the potential cellular effects of brimonidine-containing formulations on corneal cells, which is particularly relevant for glaucoma patients undergoing long-term treatment with these medications.

3. Methods

3.1. Cell Culture and Treatment

Primary human corneal keratocytes were isolated from the limbal stroma of a cornea obtained from the Central Eye Bank of Iran after its use in transplantation; the donor was a 29-year-old male cadaver. The donor had provided written informed consent for the use of their tissues in transplantation and subsequent research. All procedures were conducted in accordance with the ethical principles of the Declaration of Helsinki. This study was reviewed and approved by the Ahvaz Jundishapur University of Medical Sciences Ethics Committee (Approval Code: IR.AJUMS.REC.1402.663). It is important to note that all experiments were performed using cells from this single donor. In a sterile environment, the corneal rim was rinsed with phosphate-buffered saline (PBS, Shellmax), and its epithelial and endothelial layers were carefully scraped off. The remaining stromal tissue was minced into ~1 × 1 mm^2 explants and seeded onto a culture plate. These explants were cultured in Dulbecco's Modified Eagle Medium/Nutrient Mixture F-12 (DMEM/F12, Shellmax) supplemented with 10% fetal bovine serum (FBS, Gibco) and 1% penicillin/streptomycin (Shellmax). The culture medium was refreshed every 5 days, and cells were passaged upon reaching 80% confluency. Keratocyte identity was confirmed by verifying the expression of the markers Lumican (LUM) and Keratocan (KERA) via conventional PCR (10). For MTT and gene expression analysis, cells at passage 4 were treated with 10 µM brimonidine tartrate (0.2% ophthalmic solution, Sina Darou, Tehran, Iran) for one hour at 37 °C. The commercial formulation contains benzalkonium chloride as a preservative and other excipients. Control cells were subjected to the same procedure with a vehicle medium. The vehicle control consisted of culture medium without the drug and did not contain the same excipients or preservative as the commercial product; this difference represents a methodological limitation. The concentration of 10 µM was selected based on previous studies reporting corneal tissue concentrations of brimonidine following topical administration. The one-hour exposure was chosen to simulate the initial contact of the drug with the corneal surface, followed by a 24-hour period to assess delayed effects.

3.2. MTT Cell Viability Assay

The impact of brimonidine on keratocyte viability was quantified using the MTT (3-(4,5-dimethylthiazol-2-yl)-2,5-diphenyltetrazolium bromide) colorimetric assay. Keratocytes were seeded in 96-well plates at a density of 1×10^4 cells per well. Equal cell numbers and equivalent confluence were verified by cell counting before treatment. Following treatment, 20 µL of a 5 mg/mL MTT solution (GoldBio Co.) was added to each well. In viable cells, mitochondrial reductases convert the yellow tetrazolium salt into insoluble purple formazan crystals. After a 4-hour incubation at 37 °C, the supernatant was removed, and 100 µL of dimethyl sulfoxide (DMSO) was added to lyse the cells and solubilize the formazan. The absorbance of the resulting solution, which is proportional to the number of viable cells, was measured at 570 nm using a microplate reader (Polarstar Omega BMG LABTECH, Germany). Viability was expressed as a percentage relative to the untreated control group.

3.3. Gene Expression Analysis: Real-time PCR

Total RNA was extracted from treated and control keratocytes using the RNeasy kit (Parstous Co.). RNA quality and quantity were assessed by spectrophotometry (A260/A280 > 1.9). RNA was purified using a silica-column extraction kit. Primers were BLAST-checked and designed to avoid genomic DNA amplification; therefore, no DNase treatment was performed. Total RNA (1 µg) was reverse transcribed into complementary DNA (cDNA) using a cDNA synthesis kit (Parstous Co.) according to the manufacturer's instructions. The relative expression of

target genes was quantified by real-time PCR using a Magnetic Induction Cycler (Mic qPCR, Bio Molecular Systems). Each 10 µL PCR reaction consisted of 5 µL of RealQ_Plus Master Mix Green (Ampliqon), 1 µL of forward and reverse primers, and 4 µL of cDNA template. The thermocycling protocol included an initial 15-minute hold at 95 °C, followed by 40 cycles of denaturation at 95 °C for 10 seconds and combined annealing and extension at 61 °C for 45 seconds (10). No-template controls (NTC) and no-RT controls were included in all PCR runs. Melt-curve analysis was performed for all primer sets to confirm single-product amplification. Primer amplification efficiencies were determined by standard-curve analysis and ranged from 90 – 110% for all primer sets. The $2^{-\Delta\Delta Ct}$ method was used to calculate relative gene expression, with β-ACT serving as the endogenous reference gene for normalization. β-ACT was selected as a reference gene based on its stable expression under various stress conditions, as previously validated in corneal cell studies. Primers for LUM, KERA, BAX, BCL2, and IL1B were designed using AllelID software (v.7.5) and validated for specificity against the NCBI database (Table 1).

3.4. Bioinformatics and Network Analysis

To situate our molecular findings within a broader biological framework, we performed an in silico protein-protein interaction (PPI) network analysis. We queried the STRING database (version 12) for high-confidence (interaction score ≥ 0.7) human protein-protein interactions associated with the terms "apoptosis" and "pyroptosis", using experiments, databases, co-expression, and text mining as evidence channels. The retrieval was performed in September 2024. A total of 175 apoptosis-associated proteins and 27 pyroptosis-associated proteins were identified based on high-confidence interactions. The resulting interaction data were imported into Cytoscape software (version 3.10.3) and merged to construct a unified cell death network. Key topological properties of this network (degree, betweenness centrality, closeness centrality, stress, etc.) were calculated using the Network Analyzer tool. We then used the MCODE plugin (version 2.0), with a scoring cutoff of 4, to identify densely interconnected clusters. Finally, the network properties of the proteins of interest (BAX, BCL2, and IL1B) were analyzed in detail. This in silico network analysis is hypothesis-generating and provides a systems-level context for interpreting our experimental findings. It does not confirm that these networks were activated by the brimonidine formulation.

3.5. Statistical Analysis

A total of n = 3 independent biological experiments were conducted on separate occasions using a single donor-derived culture. Data are presented as mean ± standard error of the mean (SEM). Statistical comparisons were made using an unpaired t-test in GraphPad Prism (version 6). For the MTT assay, a single planned comparison was made between control and brimonidine-treated cells; therefore, an unpaired two-tailed t-test was used, and no multiplicity adjustment was applied. For RT-qPCR, control and brimonidine groups were compared using unpaired two-tailed t-tests because observations came from independent preparations rather than matched samples. A paired or hierarchical analysis was not used because the experimental design did not involve repeated measurements within the same preparation.

Statistical testing for RT-qPCR was performed on fold-change values ($2^{-\Delta\Delta Ct}$), as in our previous in vitro studies, rather than directly on ΔCt values. Effect sizes (Hedges' g) and 95% confidence intervals for mean differences are reported in the Results. A two-sided $P < 0.05$ was considered statistically significant. P values were interpreted as continuous measures together with effect sizes, confidence intervals, and biological context. Formal normality and equal-variance testing were not performed because n = 3 per group provides limited power for reliable assumption testing.

4. Results

4.1. The Brimonidine Formulation Altered Keratocyte Morphology and Reduced Cell Density

The cells isolated from corneal explants proliferated successfully and displayed the spindle-shaped, fibroblastic morphology characteristic of keratocytes. Their identity was confirmed by the expression of the keratocyte markers LUM and KERA (11). Visual inspection after treatment showed that keratocytes exposed to the brimonidine formulation had visibly reduced cell density compared with the confluent cell layer in the untreated control group, providing an initial qualitative indication of the formulation's cytotoxicity (Figure 1).

4.2. The Brimonidine Formulation Significantly Impaired Keratocyte Viability

The cytotoxic effect of brimonidine was quantitatively confirmed by an MTT assay. As illustrated in Figure 2, treatment with the brimonidine formulation resulted in a significant reduction in keratocyte viability of 26.19% compared with the control group (73.81 ± 1.39% vs. 100 ± 2.38%; mean difference = −26.19%; 95% CI: [−33.84, −18.54]; unpaired t-test P = 0.0007; Hedges' g = −6.21).

Table 1. Primer Sequences Used for Real-time PCR Analysis

Genes	Forward Primer (5'→3')	Reverse Primer (5'→3')	Product Size (bp)
IL1B	AGCAACAAGTGGTGTTCTCC	TGGGATCTACACTCTCCAGC	153
BAX	TTCTGACGGCAACTTCAACTGG	CACAGGGCCTTGAGCACC	78
BCL2	CCCGCGACTCCTGATTCATT	CAGTCTACTTCCTCTGTGATGTTGT	167
LUM	CTGGCTGATAGTGGAATACC	TTGATCTTGGAGTAGGATAATGG	200
KERA	CAACTGTCGCACAATCAAC	GAAGATGAGGTCCATAACTGAA	166
β-ACT	GCCTCGCCTTTGCCGAT	CATGCCGGAGCCGTTGT	98

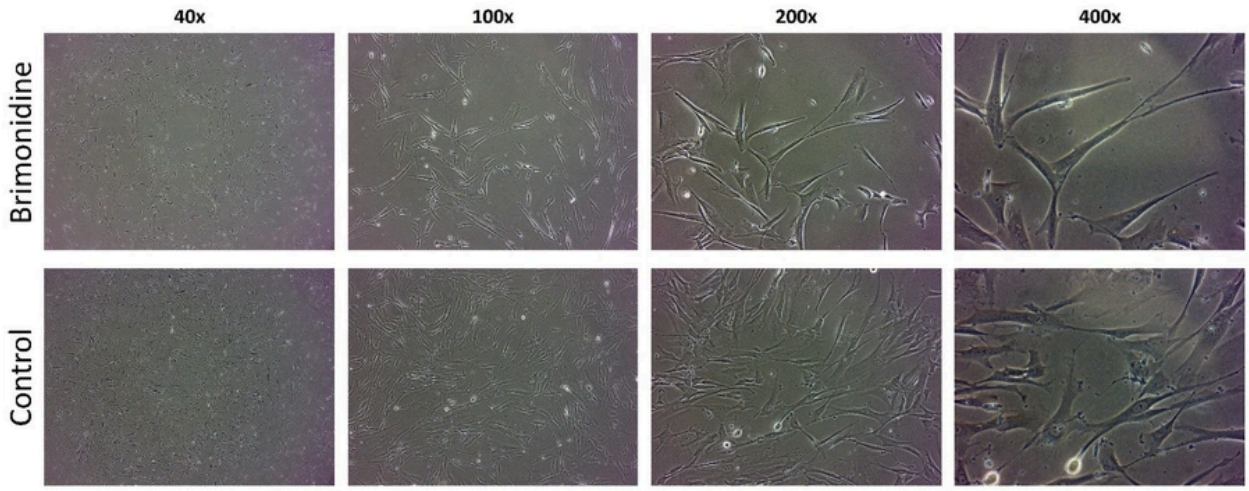

Figure 1. The Brimonidine Formulation Treatment Alters Keratocyte Morphology and Reduces Cell Density. Data represents n = 3 independent biological experiments conducted on separate occasions from a single donor-derived culture. Representative phase-contrast microscopy images of human corneal keratocytes. The top panel displays cells treated with brimonidine, while the bottom panel shows the untreated control group. Images are presented at increasing magnifications (from left to right: 40x, 100x, 200x, and 400x). Across all magnifications, the treated cells exhibit a clear reduction in cell density and a more stressed morphology compared to the confluent monolayer of healthy, spindle-shaped cells in the control group.

4.3. The Brimonidine Formulation Upregulated the Expression of Key Apoptosis and Pyroptosis-Associated Genes

Following treatment of keratocytes with the brimonidine formulation, we quantified the expression of key cell death genes. As shown in Figure 3, the formulation led to significant upregulation of the pro-apoptotic gene BAX (26.34 ± 5.12 vs. control set to 1.00; mean difference = 25.34; 95% CI [11.13, 39.55]; P = 0.0078; Hedges' g = 3.23) and the pyroptosis-associated inflammatory gene IL1B (5.12 ± 1.20; mean difference = 4.12; 95% CI [0.79, 7.45]; P = 0.0268; Hedges' g = 2.24) compared with controls. The anti-apoptotic gene BCL2 also increased, but this change did not reach statistical significance (8.69 ± 3.14; mean difference = 7.69; 95% CI [−1.03, 16.41]; P = 0.0706; Hedges' g = 1.60). Importantly, the BCL2/BAX ratio showed a decreasing trend; however, this change did not reach statistical significance (P = 0.0641; Figure 4).

4.4. How BCL2, BAX, and IL1B Are Integrated into the Apoptosis/Pyroptosis Network

To create a comprehensive map of the cell death machinery, our biophysical analysis began with the construction of distinct PPI networks for apoptosis and pyroptosis. The apoptosis network comprised 175 protein nodes linked by 2,858 interactions (edges). The pyroptosis network, comprising 27 nodes and 179 edges, was also constructed. The two networks were then merged to create a global, systems-level view of the cell death interactome. The final integrated network comprised 192 nodes and 2,969 interactions, with a global clustering coefficient of 0.712 and a network density of 0.162. Figure 5 shows the

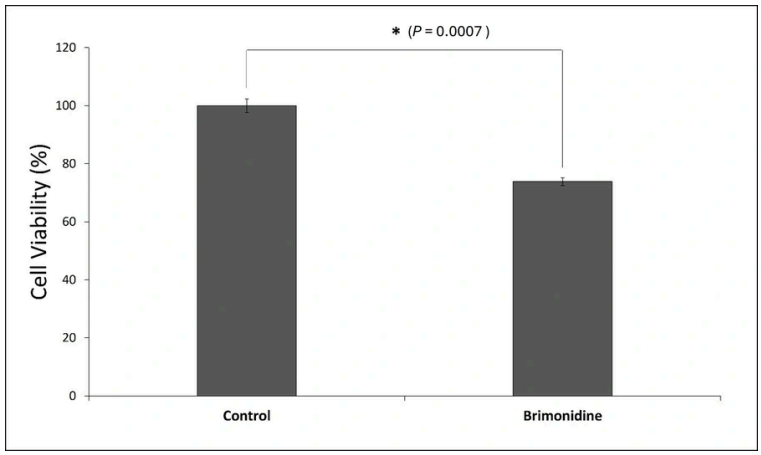

Figure 2. The Brimonidine Formulation Significantly Reduces Keratocyte Viability. Data are presented as mean ± SEM (n = 3 independent biological experiments conducted on separate occasions from a single donor-derived culture). *P = 0.0007 vs. control, as determined by an unpaired t-test (mean difference = −26.19%; 95% CI: [−33.84, −18.54]; Hedges' g = −6.21).

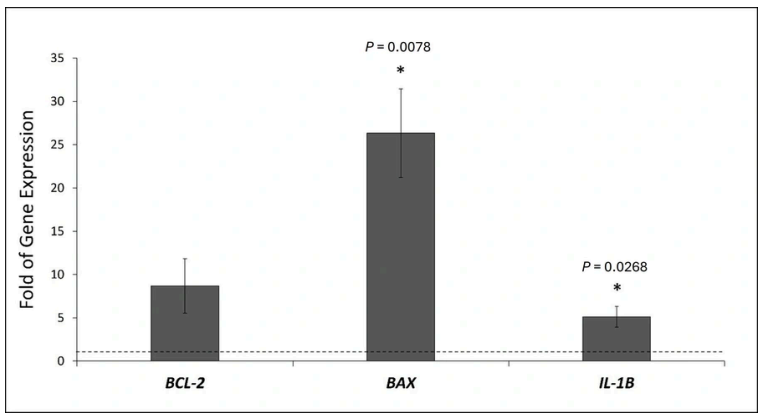

Figure 3. The Brimonidine Formulation Upregulates Pro-Apoptotic and Pyroptosis-Associated Inflammatory Gene Expression. Data are presented as mean ± SEM (n = 3 independent biological experiments conducted on separate occasions from a single donor-derived culture). *P = 0.0078 for BAX; *P = 0.0268 for IL1B vs. control, unpaired t-test. BCL2: P = 0.0706 (not statistically significant). 95% CI for BAX fold-change: 11.13, 39.55; for IL1B fold-change: 0.79, 7.45; for BCL2 fold-change: −1.03, 16.41.

merged PPI network for apoptosis and pyroptosis. The BAX, BCL2 (cluster 2), and IL1B (cluster 7) nodes are highlighted by red circles in the network.

Using the MCODE algorithm, we identified 8 densely interconnected clusters within this network. Specifically, BCL2 and BAX were co-localized within Cluster 2 (31 nodes, 394 edges, score = 26.267), consistent with their established functional partnership in regulating apoptosis. IL1B was a key component of Cluster 7 (18 nodes, 39 edges, score = 4.588), a distinct module representing the inflammatory arm of programmed cell death.

The analysis of the individual protein properties (Supplementary Table 1) further underscored their importance and indicated that BCL2, BAX, and IL1B were structurally important nodes based on multiple centrality metrics. BCL2 showed a high degree of 70, placing it among the most connected proteins in the network, along with elevated betweenness centrality (0.031) and closeness

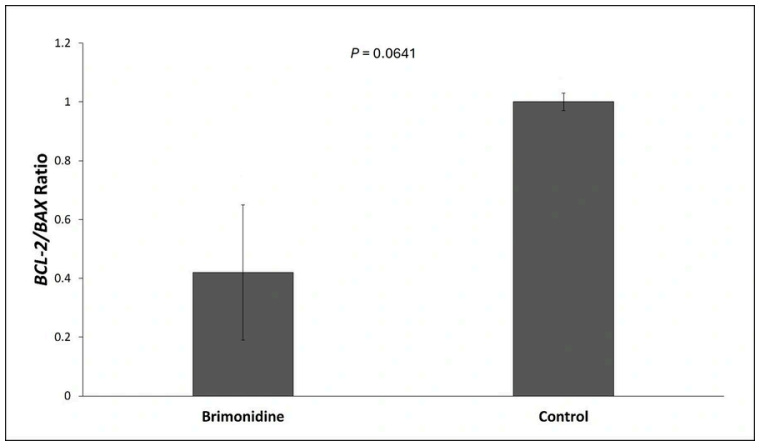

Figure 4. Brimonidine Induces a Pro-Apoptotic Shift in the BCL2/BAX Ratio. The BCL2/BAX expression ratio, a key indicator of apoptotic propensity, was calculated from the gene expression data. Treatment with brimonidine resulted in a decreased ratio, a shift trend towards a pro-apoptotic state in keratocytes, however the difference was not statistically significant (P = 0.0641). Data are presented as mean ± SEM (n = 3 independent biological experiments conducted on separate occasions from a single donor-derived culture).

centrality (0.612), indicating a prominent role in information flow and global network integration. BCL2 also exhibited a high stress value (13,560), reflecting frequent participation in shortest paths, and was assigned to Cluster 2, corresponding to the core apoptotic module. In contrast, BAX displayed a degree of 39, moderate betweenness centrality (0.0034), and closeness centrality of 0.541, suggesting a well-connected but less globally controlling position. BAX showed a substantial stress value of 1,520 and a higher clustering coefficient (0.584), consistent with its embedding in a tightly interconnected apoptotic subnetwork within the same cluster.

IL1B exhibited a distinct topological profile characterized by moderate connectivity (degree = 15) and lower betweenness centrality (0.0017), but relatively high closeness centrality (0.509) and stress (1,562), indicating frequent participation in localized signaling paths. Notably, IL1B showed a high clustering coefficient (0.714) and was assigned to Cluster 7, an inflammation- and inflammasome-associated module. These quantitative differences demonstrate that BCL2 functions as a global apoptotic hub and bottleneck, BAX as a clustered execution-level node within the apoptotic core, and IL1B as a locally central inflammatory mediator within the pyroptosis network. It is important to emphasize that this network analysis describes the topology of known protein-protein interactions from database sources and is hypothesis-generating; it does not demonstrate that these networks were activated by the brimonidine formulation in our experimental system.

5. Discussion

Brimonidine is a well-known drug for managing IOP in glaucoma. However, its widespread and long-term use is often complicated by ocular surface side effects. Our study provides a potential molecular explanation for these clinical observations by demonstrating that a commercial brimonidine formulation induces transcriptional changes consistent with programmed cell death pathways in human corneal keratocytes.

We found that the brimonidine formulation significantly reduces keratocyte viability, a finding that resonates with broader clinical evidence that chronic use of topical glaucoma medications can compromise the health of the ocular surface (12). The observed keratocyte cytotoxicity is particularly concerning, as these cells are essential for corneal repair and transparency. Keratocyte cytotoxicity can lead to a significant risk for glaucoma patients who are already managing a chronic, vision-threatening disease. However, it is important to note that our experiments were performed using cells from a single donor, and the tested formulation contained preservatives and excipients that may have contributed to the observed effects.

Our molecular data reveal that the brimonidine formulation upregulates BAX, a key executioner in the intrinsic apoptotic pathway. Once activated, BAX triggers mitochondrial outer membrane permeabilization and apoptotic cell death (13). In response to this pro-death signal, the cells appear to increase a weak protective

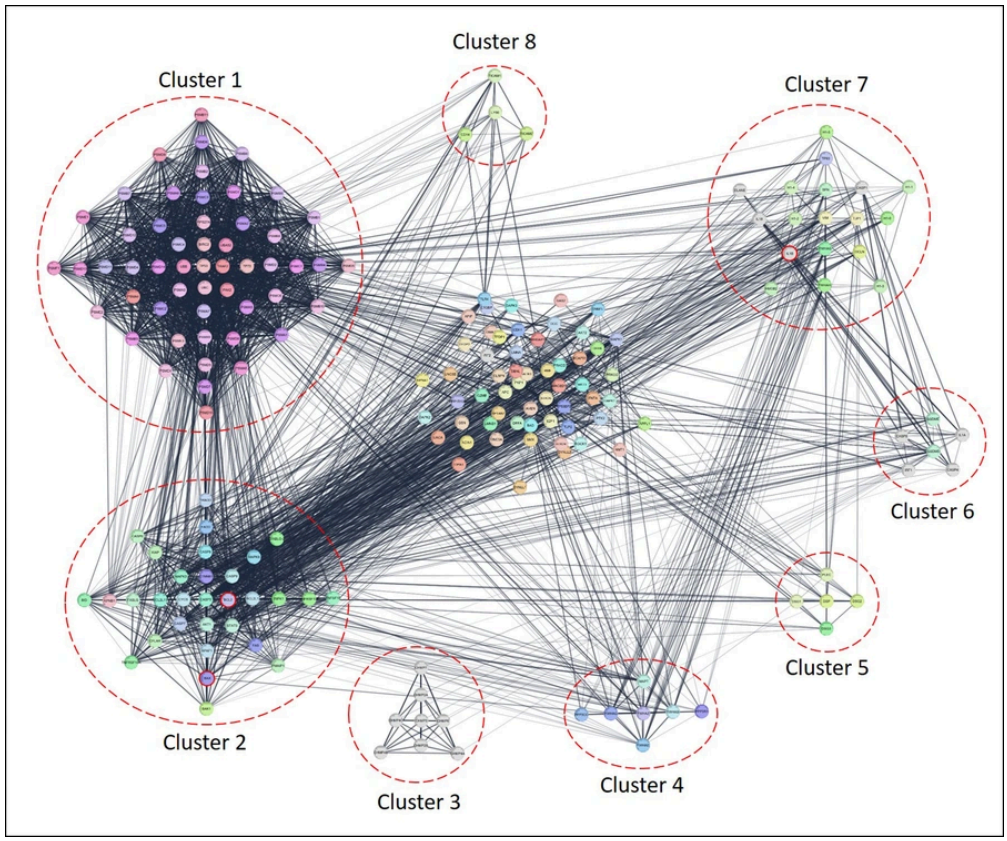

Figure 5. Integrated Protein-Protein Interaction (PPI) Network of Apoptosis and Pyroptosis. The merged interactome illustrates the systems-level organization of programmed cell death, with key nodes highlighted. BCL2 and BAX (Cluster 2) and IL1B (Cluster 7) are marked in red, representing central apoptotic and inflammatory/pyroptotic modules, respectively. Densely connected clusters were identified by MCODE analysis; quantitative network properties and detailed analyses are provided in the text. Nodes are arranged according to degree centrality, and edge thickness indicates interaction confidence scores from STRING. This network analysis is derived from database sources and is hypothesis-generating; it does not demonstrate that these networks were activated in our experimental system.

counter-attack by marginally increasing the expression of the anti-apoptotic BCL2, that can be interpreted as a cellular stress response, where pro-survival pathways are activated in an attempt to counteract overwhelming pro-death stimuli (14). Our results show that BCL2/BAX ratio has been decreased, suggesting that the brimonidine formulation may push keratocytes over the apoptotic threshold. However, it is important to emphasize that increased BAX expression and a reduced BCL2/BAX ratio are transcriptional indicators of apoptotic signaling and do not constitute direct evidence of apoptosis. The BCL2/BAX ratio result (P = 0.0641) did not reach statistical significance and should be interpreted with caution. Definitive confirmation of apoptosis requires functional assays such as Annexin V staining, TUNEL assay, caspase activity measurements, or mitochondrial membrane potential assessment. In addition, the observed increase in BCL2 expression did not reach statistical significance (P = 0.0706). Our findings may be interpreted as evidence supporting previous reports on other ocular medications that have been shown to disrupt this critical balance (15).

IL1B was the other gene investigated in this study. IL1B is a potent pro-inflammatory cytokine and a defining hallmark of pyroptosis, a highly inflammatory form of programmed cell death driven by inflammasomes (16). Pyroptosis is increasingly recognized as a key player in various ocular pathologies, including glaucoma itself (17, 18). Pyroptosis results in the release of inflammatory cellular contents, which can trigger a self-perpetuating cycle of inflammation and further cell death (19, 20). The induction of IL1B by the brimonidine formulation suggests that the drug may trigger not only apoptotic cell death but

also an inflammatory cell death response that may be consistent with pyroptotic signaling. However, it is critical to note that IL1B mRNA upregulation alone does not demonstrate pyroptosis. Pyroptosis requires evidence of inflammasome activation, caspase-1 activity, gasdermin D cleavage, release of mature IL1B, and lytic cell death. The increased IL1B expression we observed could also reflect a non-pyroptotic inflammatory stress response. This inflammatory component could contribute to the chronic ocular surface irritation and discomfort frequently reported by patients receiving long-term brimonidine therapy. Moreover, inflammasome activation and IL1B release have been mechanistically linked to mitochondrial dysfunction (21), suggesting potential crosstalk between the apoptotic and pyroptotic pathways initiated by brimonidine.

From a systems-level perspective, the network positions of BCL2, BAX, and IL1B suggest that cell fate regulation within the apoptosis/pyroptosis continuum is controlled by hierarchical and modular interactions rather than by isolated gene activity. The high centrality and bottleneck characteristics of BCL2 imply that it exerts broad regulatory control over mitochondrial apoptosis and indirectly influences downstream inflammatory death pathways. BAX, embedded within a densely connected apoptotic cluster, represents a critical convergence point for pro-death signaling, translating upstream regulatory inputs into irreversible mitochondrial commitment. Meanwhile, IL1B's localization within a highly clustered inflammatory subnetwork highlights its role as a signal amplifier in pyroptotic and immune-associated cell death, as well as its crosstalk with apoptotic modules. Together, these bioinformatic findings indicate that coordinated regulation of these genes can propagate effects across multiple death pathways, providing a mechanistic explanation for how perturbations at a small number of strategically positioned nodes may reshape global apoptosis/pyroptosis network behavior and ultimately determine cell fate.

In summary, our data suggest that the commercial brimonidine formulation induces transcriptional changes related to keratocyte cell death through at least two distinct but coordinated pathways: apoptotic and inflammatory signaling, which may be consistent with apoptosis and pyroptosis. This transcriptional signature raises questions about the potential long-term consequences of brimonidine-containing formulations for corneal health. Chronic inflammation and a depleted keratocyte population can severely impair the cornea's wound-healing capabilities, potentially leading to scarring, thinning, and loss of transparency (22). These findings underscore the need for further investigation into the clinical implications of brimonidine's effects, particularly in patients using the drug for extended periods.

5.1. Limitations

This study has several important limitations. First, all experiments were performed using keratocytes isolated from a single 29-year-old male donor. This limits the generalizability of our findings, and validation using cells from multiple independent donors is essential before broader conclusions can be drawn. Second, the tested intervention was a commercial brimonidine tartrate ophthalmic solution containing benzalkonium chloride as a preservative and other excipients. The vehicle control consisted of culture medium without the drug and did not contain the same excipients or preservative. Therefore, the observed cytotoxic effects cannot be attributed exclusively to brimonidine itself and may be partially or fully related to other formulation components. Third, only a single concentration (10 µM) and a single exposure duration (one hour) were tested; the absence of dose-response and time-course data limits the translational relevance of our findings. Fourth, the MTT assay measures mitochondrial metabolic activity and does not distinguish among reduced metabolic activity, decreased cell number, growth inhibition, or different modes of cell death. Fifth, the study did not include direct functional assays to confirm apoptosis (e.g., Annexin V staining, TUNEL assay, caspase activity) or pyroptosis (e.g., cleaved gasdermin D, caspase-1 activity, mature IL1B release). Therefore, our findings represent transcriptional changes consistent with apoptotic and inflammatory signaling rather than confirmed apoptosis or pyroptosis. Future studies addressing these limitations are necessary to definitively establish the mechanisms of brimonidine-induced keratocyte cytotoxicity.

5.2. Conclusions

This study demonstrated that a commercial brimonidine tartrate ophthalmic formulation exerts a significant cytotoxic effect on human corneal keratocytes. The formulation disrupts the balance of gene expression by upregulating the pro-apoptotic marker BAX and the pyroptosis-associated inflammatory cytokine IL1B. The BCL2/BAX ratio showed a decreasing trend; however, this change did not reach statistical significance. These data suggest that, despite its therapeutic efficacy in lowering IOP, brimonidine-containing formulations may have unintended off-target effects on corneal health by promoting transcriptional changes consistent with apoptotic and inflammatory cell death pathways. Further research is needed to understand the clinical relevance of these findings and to develop strategies to mitigate the

potential long-term cytotoxic effects of this medication. Specifically, future studies using cells from multiple donors, purified brimonidine with matched vehicle controls, dose-response designs, and orthogonal functional assays for apoptosis and pyroptosis are necessary to confirm and extend these preliminary observations.

Acknowledgements

The authors thank the directors of Ahvaz Jundishapur University of Medical Sciences and Shiraz University of Medical Sciences for supporting this research.

Footnotes

AI Use Disclosure: The authors declare that no generative AI tools were used in the preparation of this article.

Authors' Contribution: A. S. designed the study, performed the in vitro tests, and drafted the manuscript. F. SJ. performed the bioinformatic analysis, contributed to the in vitro tests and data acquisition, and revised the article. M. S. contributed to the in vitro tests and data acquisition. A. M. contributed to data analysis and interpretation. R. K. contributed to the literature review and manuscript preparation. M. A. designed and supervised the study and finalized the manuscript. All authors read and approved the final manuscript.

Conflict of Interests Statement: The authors declare that they have no conflicts of interest.

Data Availability: The data supporting the findings of this study are available from the corresponding author upon request.

Ethical Approval: This study was approved by the Ethics Committee of Ahvaz Jundishapur University of Medical Sciences (IR.AJUMS.REC.1402.663).

Funding/Support: This study was supported by Ahvaz Jundishapur University of Medical Sciences and Shiraz University of Medical Sciences.

Informed Consent: The donor provided written informed consent for the use of their tissues in transplantation and subsequent research.

References

1. Cantor LB. Brimonidine in the treatment of glaucoma and ocular hypertension. *Ther Clin Risk Manag*. 2006;**2**(4):337-346. [PubMed ID: 18360646]. [PubMed Central ID: PMC1936355]. https://doi.org/10.2147/tcrm.2006.2.4.337.
2. Lee JS, Kim CY. Brimonidine tartrate ophthalmic solution 0.025% for redness relief: An overview of safety and efficacy. *Expert Rev Clin Pharmacol*. 2022;**15**(8):911-919. [PubMed ID: 35951740]. https://doi.org/10.1080/17512433.2022.2112948.
3. Cimolai N. A review of neuropsychiatric adverse events from topical ophthalmic brimonidine. *Hum Exp Toxicol*. 2020;**39**(10):1279-1290. [PubMed ID: 32347114]. https://doi.org/10.1177/0960327120918307.
4. Maciulaitiene R, Kalesnykas G, Pauza DH, Januleviciene I. A combination of topical and systemic administration of brimonidine is neuroprotective in the murine optic nerve crush model. *PLoS One*. 2024;**19**(8):e0308671. [PubMed ID: 39116180]. [PubMed Central ID: PMC11309405]. https://doi.org/10.1371/journal.pone.0308671.
5. Galanopoulos A, Goldberg I. Clinical efficacy and neuroprotective effects of brimonidine in the management of glaucoma and ocular hypertension. *Clin Ophthalmol*. 2009;**3**:117-122. [PubMed ID: 19668554]. [PubMed Central ID: PMC2709013]. https://doi.org/10.2147/opth.s3270.
6. Torricelli AA, Wilson SE. Cellular and extracellular matrix modulation of corneal stromal opacity. *Exp Eye Res*. 2014;**129**:151-160. [PubMed ID: 25281830]. [PubMed Central ID: PMC4259857]. https://doi.org/10.1016/j.exer.2014.09.013.
7. Massoudi D, Malecaze F, Galiacy SD. Collagens and proteoglycans of the cornea: Importance in transparency and visual disorders. *Cell Tissue Res*. 2016;**363**(2):337-349. [PubMed ID: 26205093]. https://doi.org/10.1007/s00441-015-2233-5.
8. Wong HL, Poon SHL, Bu Y, Lo ACY, Jhanji V, Chan YK, et al. A systematic review on cornea epithelial-stromal homeostasis. *Ophthalmic Res*. 2021;**64**(2):178-191. [PubMed ID: 32474566]. https://doi.org/10.1159/000509030.
9. Acheampong AA, Shackleton M, John B, Burke J, Wheeler L, Tang-Liu D. Distribution of brimonidine into anterior and posterior tissues of monkey, rabbit, and rat eyes. *Drug Metab Dispos*. 2002;**30**(4):421-429. [PubMed ID: 11901096]. https://doi.org/10.1124/dmd.30.4.421.
10. Sanie-Jahromi F, Sadeghi N, Moayedfard Z, Gharegezloo Z, Nejabat M, Nowroozzadeh MH. Effects of exosomes derived from activated corneal stromal keratocytes on the inflammation, proliferation, neuroprotection and epithelial-mesenchymal transition in retinal pigment epithelium cells. *Life Sci*. 2025;**371**:123592. [PubMed ID: 40174671]. https://doi.org/10.1016/j.lfs.2025.123592.
11. Sanie-Jahromi F, Mohsenzadeh AH, Namjoyan F, Gharegezloo Z, Nejabat M. Effect of adlay seed extract on inflammation and fibrogenesis in human corneal activated keratocytes at transcriptional level. *Exp Eye Res*. 2023;**235**:109641. [PubMed ID: 37696465]. https://doi.org/10.1016/j.exer.2023.109641.
12. Kucukoduk A, Durmus IM, Aksoy M, Karakurt S. Cytotoxic, apoptotic, and oxidative effects of preserved and preservative-free brimonidine in a corneal epithelial cell line. *J Ocul Pharmacol Ther*. 2022;**38**(8):576-583. [PubMed ID: 36178959]. https://doi.org/10.1089/jop.2022.0053.
13. Youle RJ, Strasser A. The BCL-2 protein family: Opposing activities that mediate cell death. *Nat Rev Mol Cell Biol*. 2008;**9**(1):47-59. [PubMed ID: 18097445]. https://doi.org/10.1038/nrm2308.
14. Danial NN, Korsmeyer SJ. Cell death: Critical control points. *Cell*. 2004;**116**(2):205-219. [PubMed ID: 14744432]. https://doi.org/10.1016/s0092-8674(04)00046-7.
15. Carnevale C, Riva I, Roberti G, Michelessi M, Tanga L, Verticchio Vercellin AC, et al. Confocal microscopy and anterior segment optical coherence tomography imaging of the ocular surface and bleb morphology in medically and surgically treated glaucoma patients: A review. *Pharmaceuticals (Basel)*. 2021;**14**(6):581. [PubMed ID: 34207162]. [PubMed Central ID: PMC8234834]. https://doi.org/10.3390/ph14060581.

16. Wu J, Nguyen H, Simonette R, Rady P, Tyring S. Innate immunity, inflammation & microbiology. *J Invest Dermatol*. 2015;**135**:S87-98.
17. Kesavardhana S, Malireddi RKS, Kanneganti TD. Caspases in cell death, inflammation, and pyroptosis. *Annu Rev Immunol*. 2020;**38**(1):567-595. [PubMed ID: 32017655]. [PubMed Central ID: PMC7190443]. https://doi.org/10.1146/annurev-immunol-073119-095439.
18. Chen D, Miao S, Chen X, Wang Z, Lin P, Zhang N, et al. Regulated necrosis in glaucoma: Focus on Ferroptosis and Pyroptosis. *Mol Neurobiol*. 2024;**61**(5):2542-2555. [PubMed ID: 37910286]. https://doi.org/10.1007/s12035-023-03732-x.
19. Lu L, Zhang Y, Tan X, Merkher Y, Leonov S, Zhu L, et al. Emerging mechanisms of pyroptosis and its therapeutic strategy in cancer. *Cell Death Discov*. 2022;**8**(1):338. [PubMed ID: 35896522]. [PubMed Central ID: PMC9329358]. https://doi.org/10.1038/s41420-022-01101-6.
20. Hachim MY, Khalil BA, Elemam NM, Maghazachi AA. Pyroptosis: The missing puzzle among innate and adaptive immunity crosstalk. *J Leukoc Biol*. 2020;**108**(1):323-338. [PubMed ID: 32083338]. https://doi.org/10.1002/JLB.3MIR0120-625R.
21. Tang L, Xu GT, Zhang JF. Inflammation in diabetic retinopathy: Possible roles in pathogenesis and potential implications for therapy. *Neural Regen Res*. 2023;**18**(5):976-982. [PubMed ID: 36254977]. [PubMed Central ID: PMC9827774]. https://doi.org/10.4103/1673-5374.355743.
22. Dohlman CH, Zhou C, Lei F, Cade F, Regatieri CV, Črnej A, et al. Glaucoma after corneal trauma or surgery—a rapid, inflammatory, IOP-independent pathway. *Cornea*. 2019;**38**(12):1589-1594. [PubMed ID: 31453878]. [PubMed Central ID: PMC6830965]. https://doi.org/10.1097/ICO.0000000000002106.